

Comparative study between *Hfe*^{-/-} and *β2m*^{-/-} mice: progression with age of iron status and liver pathology

Pedro Rodrigues^{*†}, Célia Lopes[†], Claudia Mascarenhas^{*}, Paolo Arosio[‡], Graça Porto^{*§} and Maria De Sousa^{*†}

^{*}Iron Genes and Immune System (IRIS), Institute for Molecular and Cell Biology (IBMC), Porto, Portugal, [†]Molecular Pathology and Immunology, Abel Salazar for Biomedical Sciences (ICBAS), Porto, Portugal, [‡]Genomics for the Diagnosis of Human Pathologies Unit (IRCCS H), San Raffaele, Milan, Italy, and [§]Hematology, Santo António General Hospital (HGSA), Porto, Portugal

INTERNATIONAL JOURNAL OF EXPERIMENTAL PATHOLOGY

Summary

Hepatic iron overload in hemochromatosis patients can be highly variable but in general it develops in older patients. The purpose of this study was to compare development of iron load in of *β2m*^{-/-} and *Hfe*^{-/-} mice paying special attention to liver pathology in older age groups. Liver iron content of *β2m*^{-/-}, *Hfe*^{-/-} and control B6 mice of different ages (varying from 3 weeks to 18 months) was examined. Additional parameters (haematology indices, histopathology, lipid content and ferritin expression) were also studied in 18-month-old mice. The *β2m*^{-/-} strain presents higher hepatic iron content, hepatocyte nuclear iron inclusions, mitochondria abnormalities. In addition, hepatic steatosis was a common observation in this strain. In the liver of *Hfe*^{-/-} mice, large mononuclear infiltrates positive for ferritin staining were commonly observed. The steatosis commonly observed the *β2m*^{-/-} mice may be a reflection of its higher hepatic iron content. The large hepatic mononuclear cell infiltrates seen in *Hfe*^{-/-} stained for ferritin, may point to the iron sequestration capacity of lymphocytes and contribute to the clarification of the differences found in the progression of hepatic iron overload and steatosis in older animals from the two strains.

Keywords

β2m, *Hfe*, iron overload, lymphocytes, steatosis

Received for publication:
8 March 2006
Accepted for publication:
11 May 2006

Correspondence:

Pedro Rodrigues, MSc, PhD
Iron Genes and Immune System,
IBMC
Rua do Campo Alegre 823
4150-180 Porto
Portugal
Tel.: +351 226074956;
Fax: +351 226098480;
E-mail: prodrigu@ibmc.up.pt

β2m^{-/-} mice develop spontaneously hepatic iron overload with a distribution similar to that seen in the liver pathology of hereditary hemochromatosis (HH). They have become thus an excellent model for the study of iron overload disorders (De Sousa *et al.* 1994; Rothenberg & Voland 1996; Santos *et al.* 1996). With the discovery of the *Hfe* gene (a non-classical MHC class I gene) and the demonstration that the C282Y mutated form failed to bind to *β2m* (Feder *et al.* 1996), the explanation for the earlier findings in *β2m*

KO mice was thought to lie in the impairment of *Hfe* function due to the lack of expression of the *β2m* molecule. However, subsequent studies of iron overload models in KO mice showed that this was insufficient to explain the pathology of *β2m*^{-/-} mice. Mice double knockout (KO) for *Hfe* and *β2m* accumulate more tissue iron than KO mice for *Hfe* alone (Levy *et al.* 2000). *Mhc* class I Knockout animals have also higher liver iron levels, demonstrating the involvement of classical MHC class I molecules in the regulation of iron

metabolism. The existence of additional $\beta 2m$ interacting molecules implicated in the regulation of iron absorption was further demonstrated by Miranda *et al.* (2004) showing that $\beta 2mRag1(-/-)$ and $HfeRag1(-/-)$ have an exceptionally high-iron overload status. In addition, the analysis of the differential gene expression of genes involved in iron metabolism in $\beta 2m-/-$ and $Hfe-/-$ mice using a specialized IronChip cDNA-based microarray revealed differences in iron gene expression profiles (Muckenthaler *et al.* 2003, 2004) between the two models. Although the increased expression of the duodenal iron transporters (DMT-1 and ferroportin 1), found by Muckenthaler *et al.* (2004), may explain the documented increase in iron absorption in $\beta 2m-/-$ mice (Santos *et al.* 1996), a similar situation was not observed in $Hfe-/-$ mice with the same genetic background (Herrmann *et al.* 2004). Low hepcidin expression was also documented in that study in the $\beta 2m$ KO mice.

The majority of the studies carried out with animal models of iron overload have used young adult mice. Age, however, is a critical factor in the expression of HH and other iron overload disorders often associated with related liver disease in humans. In the present paper, we present the results of a comparative study of two models of spontaneous iron overload in mice older than 12 months. The models examined are $\beta 2m-/-$ and $Hfe-/-$ mice kept on a normal diet. The study focuses on liver pathology and reveals differences in patterns of iron distribution within cells, in lipid accumulation and in mononuclear cell infiltration.

Animals, materials and methods

Mice

The $\beta 2m-/-$, $Hfe-/-$ mice (both backcrossed onto B6 background) and C57Bl/6 (B6) mice were bred and housed at the Institute for Molecular and Cell Biology (IBMC) animal facility. Mice used in this study were from several age groups (3 weeks, 3.5 months, 9 months and 18 months) and were fed with standard diet *ad libitum*. For the haematological parameters six to eight animals of the oldest age group (18 months) were killed. For the histological analysis, tissues from 11 to 18 animals were examined. All animal experiments were carried out in compliance with the animal ethics guidelines at the institute.

Histology and electron microscopy

Samples of liver, spleen and pancreas of 18-month-old mice [$B6$, $Hfe-/-$ and $\beta 2m-/-$] were fixed in buffered formaldehyde. After routine histology, the paraffin sections were stained by

haematoxylin–eosin. Ferric iron was detected by Perls' blue staining.

For the electron microscopy, small pieces of liver from the same animal groups were fixed in 2.5% glutaraldehyde (v/v) in cacodylate buffer (0.1 M, pH 7.2) for at least 24 h at 4°C. The tissue was washed twice with cacodylate buffer and post-fixed in 1% (w/v) OsO_4 in the same buffer. The samples were embedded in Epon resin (TAAB Lab Equipment Ltd, Berkshire, Berkshire, UK) after dehydration in a graded series of ethanol. Semithin sections (1 μm) were performed and were stained with methylene blue. Ultrathin sections (60 nm) were cut and contrasted with 2.5% uranyl acetate followed by lead citrate. Ultrastructure analysis was done under a Zeiss EM10 electron microscope (Zeiss, Oberkochen, Germany).

Iron measurements

Briefly, liver samples from the age groups studied of the B6, $Hfe-/-$ and $\beta 2m-/-$ strains were collected and stored at $-70^\circ C$ for further use. Liver non-haeme iron was measured by the bathophenanthroline method (Torrance & Bothwell 1980).

Transferrin saturation and haematological measurements

The blood samples were obtained by cardiac puncture from 18-month-old mice [$B6$, $Hfe-/-$ and $\beta 2m-/-$] under anaesthesia. For the erythroid parameters, blood was harvested in EDTA tubes and haemoglobin, erythrocyte counts, haematocrit (HCT) and mean corpuscular volume (MCV) assessed on a Coulter-S counter (Coulter Electronics, Fullerton, CA). For Iron levels, 200 μl of serum from each animal was used to determine the serum iron and total iron binding capacity (TIBC) by the ferrozine method using a Cobas Fara chemical analyser. Transferrin saturation was calculated as (serum iron/TIBC) $\times 100$.

Liver ferritin immunohistochemistry

Liver samples were fixed in buffered formaldehyde, paraffin sections were immunostained with polyclonal antibodies for H and L mouse ferritin subunitits (P. Arosio). All sections were stained using the Avidin Biotin Complex method. Before immunohistochemical staining, slides were deparaffinized with xylene, and passed through graded alcohols and treated for epitope retrieval by incubation in a microwave oven for 20 min in EDTA 1 mM, pH 8 (759 W). The samples were placed on tris-buffered saline (TBS) and to reduce non-specific binding, normal pig serum diluted 1:5 was applied for 20 min. Subsequently, the sections were

incubated over night with polyclonal rabbit anti-Fer-H or Fer-L at a 1:100 dilution. Then, after removing the excess of serum and washing in TBS, pig anti-rabbit immunoglobulin conjugated with biotin (DAKO, Glostrup, Denmark) was applied for 30 min diluted 1:200. After additional washes, colour was developed with the dy-amine benzidine (DAB) substrate (DAKO) for 2 min. After washing, the sections were counterstained with Mayer's hematoxylin for 30 min and mounted in Aquatex® (Merck, Darmstadt, Germany).

Quantitative lipid vacuoles microscopy analyses

A Leica DMLB microscope (Leica Cambridge Ltd., Cambridge, UK) equipped with a colour charge-coupled device (CCD) camera was used to examine the liver sections under a $\times 100$ magnification. In LeicaQWin image analyser (Leica Cambridge, Ltd.) a square image frame (with an area of $26276.5 \mu\text{m}^2$) was used. For each mice, five similar (i.e. in the same zone of the section) microscopic fields, in randomly chosen hepatic lobuli, were evaluated for vacuoles. The results were expressed as the mean \pm SEM (area μm^2). Computerized image analysis of lipids content was done using a routine developed in the LeicaQWin program. Threshold levels of brightness were set and a temporary binary colour image was super-imposed on the digitalized image. The areas of interest (white) were outlined in a pseudocolour. This allows the operator to check the accuracy of the measured area. Thus, the mean of positive areas was obtained and expressed as mean \pm SEM.

Statistical analyses

All statistical analysis was done using the software MINITAB. The effect of treatment was analysed using the Mann-Whitney *U*-test with subsequent Bonferroni corrections for multiple comparisons for continuous variables and chi-square test for proportions. Results are presented as means \pm SEM. Differences were considered significant at $P < 0.05$.

Results

Liver iron content

At 3 weeks of age no significant differences were seen between control and knock-out strains (Figure 1). At 3.5 months, both the $Hfe^{-/-}$ and $\beta 2m^{-/-}$ mice had developed iron overload when compared with the B6. Between 3.5 and 9 months the $\beta 2m^{-/-}$ mice further increased the hepatic iron concentration, whereas the $Hfe^{-/-}$ maintained the value

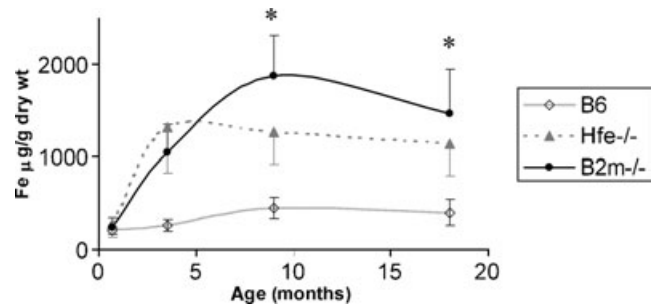


Figure 1 Hepatic iron concentration vs. age in B6, $Hfe^{-/-}$ and $\beta 2m^{-/-}$ strains. Liver samples ($n = 8-12$) were collected at 0.7, 3.5, 9 and 18 months from all strains. For the iron quantification, the bathophenanthroline method was used. *Statistically significant difference ($P < 0.05$) between the B6 strain and the $Hfe^{-/-}$ and $\beta 2m^{-/-}$ strains.

observed at 3.5 months. These differences remained in 18-month-old mice (Table 2). The kinetics of the change in hepatic iron content with age is shown in Figure 1. Both strains show a similar starting point at 3 weeks, with a rapid increase in both $Hfe^{-/-}$ and $\beta 2m^{-/-}$ strains, followed by a plateau in older $Hfe^{-/-}$ mice with further increase in iron concentration in the older $\beta 2m^{-/-}$ animals. Older $\beta 2m^{-/-}$ mice present statistically significantly higher iron content than the $Hfe^{-/-}$ counterpart (Figure 1).

Haematological indices

The evaluation of the erythroid parameters, demonstrated that the 18-month-old $\beta 2m^{-/-}$ mice had significantly higher values of red blood cells (RBC) and haemoglobin when compared with mice of the B6 or $Hfe^{-/-}$ strains (Table 1). The HCT level showed an increase from B6 to $Hfe^{-/-}$ and from $Hfe^{-/-}$ to $\beta 2m^{-/-}$. However, the MCV values were significantly higher in the $Hfe^{-/-}$ followed by the $\beta 2m^{-/-}$ that in turn were higher than the B6 (Table 1).

As expected, the serum iron and transferrin saturation levels were significantly elevated in the $Hfe^{-/-}$ and $\beta 2m^{-/-}$ mice compared with the B6 counterpart. Interestingly, the levels of TIBC were high in $\beta 2m^{-/-}$ (539 ± 46) followed by the B6 (440 ± 43) and low in the $Hfe^{-/-}$ mice (383 ± 28). The respective differences were statistically significant (Table 1).

Histology and EM

From the analysis of liver sections stained with Perls from 18-month-old mice it was clear that both $\beta 2m^{-/-}$ and $Hfe^{-/-}$ had stainable iron in hepatocytes but not in Kupffer cells,

Table 1 Haematological indices of 18-month-old mice

Strain	n	Erythroid parameters				Serum iron levels		
		RBC, $\times 10^{12}/l$	Hb, mmol/l	HCT, %	MCV, fl	SI, $\mu\text{g}/\text{dl}$	TIBC, $\mu\text{g}/\text{dl}$	Tf Sat, %
B6	8	8.12 \pm 0.37 a	12.1 \pm 0.6 a	36.0 \pm 2.0 a	44.3 \pm 0.8 a	167 \pm 32 a	440 \pm 43 a	37.8 \pm 4.8 a
<i>Hfe</i> ^{-/-}	6	8.20 \pm 0.13 a	13.1 \pm 0.3 a	39.4 \pm 1.2 b	48.0 \pm 1.0 b	329 \pm 31 b	383 \pm 28 b	87.4 \pm 1.9 b
$\beta 2m$ ^{-/-}	8	9.82 \pm 0.72 b	15.3 \pm 0.9 b	45.2 \pm 2.9 c	46.0 \pm 0.9 c	403 \pm 50 b	539 \pm 46 c	73.4 \pm 12.0 b

Values are presented as mean \pm SE.

RBC, red blood cells; Hb, haemoglobin; HCT, haematocrit; MCV, mean corpuscular volume; SI, serum iron; TIBC, total iron binding capacity; Tf Sat, transferrin saturation.

Within each column different letters indicate significant differences between groups at $P < 0.05$.

Table 2 Liver histological analysis, iron content of 18-month-old mice

Strain	n	Histological analysis				Iron
		Mononuclear infiltrates, %	Steatosis foci, %	Generalized steatosis, %	Vacuoles area, μm^2 per field	Fe, $\mu\text{g}/\text{g}$ dry wt
B6	18	7 (39) a	6 (33) a	2 (11) a	130 \pm 172 a	399 \pm 140 a
<i>Hfe</i> ^{-/-}	11	8 (72) b	3 (27) a	1 (9) a	81 \pm 75 a	1142 \pm 344 b
$\beta 2m$ ^{-/-}	15	5 (33) a	9 (60) b	7 (47) b	1782 \pm 2752 b	1468 \pm 479 c

Liver iron content and vacuoles area are presented as mean \pm SE.

Within each column different letters indicate significant differences between groups at $P < 0.05$.

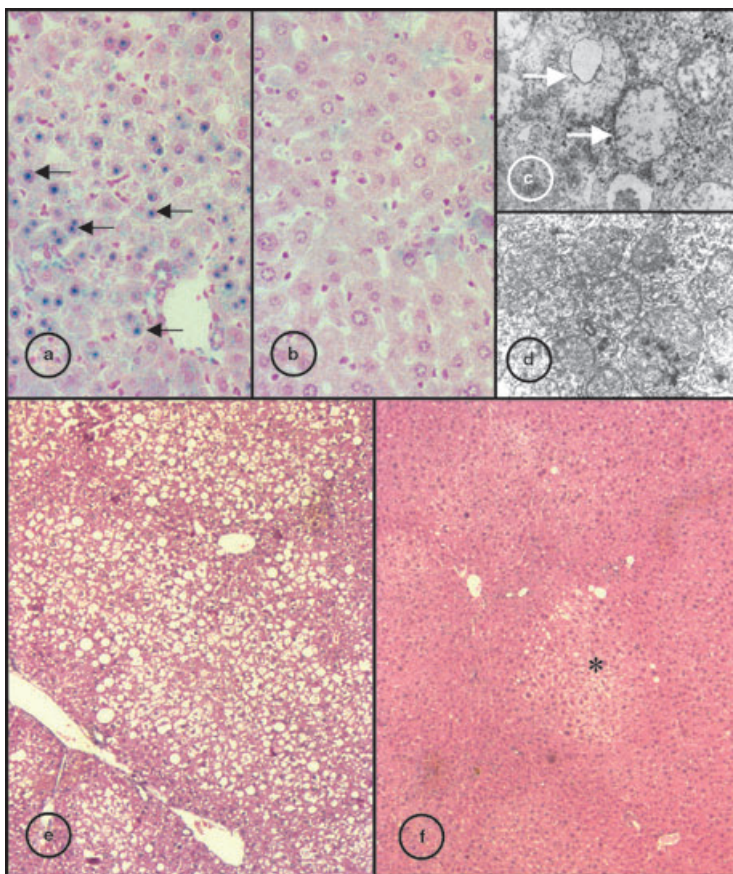
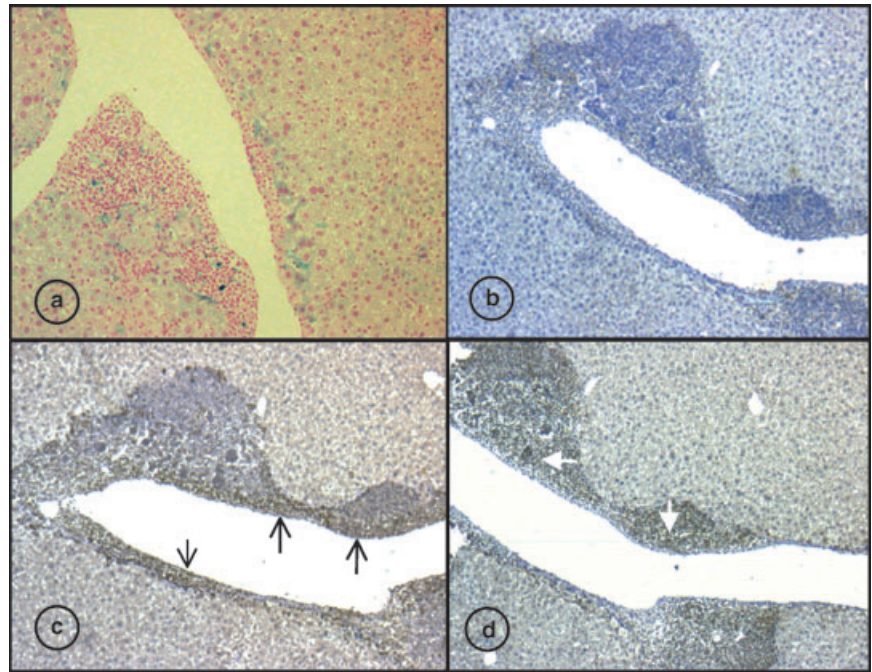


Figure 2 Liver sections of 18-month-old $\beta 2m$ and *Hfe*^{-/-} mice. Sections stained for iron by Perls method, the blue stain indicates heavy iron deposition: (a) $\beta 2m$ ^{-/-} strain, black arrow shows blue stained hepatocyte nuclear inclusions; (b) *Hfe*^{-/-} mice (original magnification $\times 400$). Electron photomicrograph of hepatic parenchyma cells; (c) $\beta 2m$ ^{-/-} mice, white arrow indicate abnormal mitochondria without visible cristae; (d) *Hfe*^{-/-} strain (original magnification $\times 8000$). Liver sections stained with HE; (e) $\beta 2m$ ^{-/-} mice, large vacuoles visible through the parenchyma indicative of generalized steatosis; (f) *Hfe*^{-/-} strain, asterisk indicate steatosis foci (original magnification $\times 40$).

Figure 3 Hepatic mononuclear infiltrates of 18-months-old $Hfe^{-/-}$ mice. (a) Liver sections stained for iron by Perls method, the dark blue stain indicates heavy iron deposition within the infiltrates (original magnification $\times 100$). (b–d) Anti-Ferritin immunohistochemistry (original magnification $\times 100$). (b) conjugate antibody only. (c) Anti-mouse Fer-L staining showing heavy Ferritin L staining in the mononuclear infiltrate endothelial region (black arrow) and in the hepatocytes. (d) Anti-mouse Fer-H staining showing a clear staining in the mononuclear infiltrates (white arrow) but not in the endothelial and parenchyma area.



indicative of an iron overload pattern similar to that of human HH, a situation not observed in the B6 mice (data not shown). However, the intensity of staining was often higher in the $\beta 2m^{-/-}$ animals when compared with the $Hfe^{-/-}$ in agreement with the iron content values (Table 2). Moreover, in the $\beta 2m^{-/-}$ mice visible blue staining in the nucleus of the hepatocytes was always seen, a situation not found in the $Hfe^{-/-}$ or B6 strains (Figure 2a,b). In addition, the ultrastructural analysis of the liver often revealed abnormal mitochondria (enlarged and without visible inner cristae) in the $\beta 2m^{-/-}$ hepatocytes (Figure 2c,d).

An analysis of liver sections showed that hepatic steatosis was more frequent in the $\beta 2m^{-/-}$ mice than in the $Hfe^{-/-}$ or B6 strains. Although steatosis foci could be observed in the three groups, the number of animals where generalized steatosis was observed, was significantly higher in $\beta 2m^{-/-}$ mice (Figure 2e,f and Table 2). Moreover, morphometric analysis of the area occupied by lipids identified by oil red stain indicative of lipid content was significantly larger in the $\beta 2m^{-/-}$ (Table 2).

The liver histology of 18-month-old mice revealed also the presence of mononuclear infiltrates often associated with large vessels. Interestingly, the frequency of mononuclear liver infiltrates on $Hfe^{-/-}$ mice was significantly higher (eight of 11 animals) when compared with $\beta 2m^{-/-}$ (5/15) or B6 (7/18) (see Table 2). In addition, it was possible to detect sporadic cells positive for Perls blue indicat-

ive of iron content in the mononuclear infiltrate (Figure 3a).

The study of heart and pancreas sections stained with Perls method showed that some of the 18-month-old $Hfe^{-/-}$ mice had cardiac iron deposits, a situation not observed in the $\beta 2m^{-/-}$ and B6 mice at similar ages.

Immunohistochemistry

To answer the question whether the presence of the mononuclear cells could be associated with the differences observed in the iron content changes seen between $\beta 2m^{-/-}$ and the $Hfe^{-/-}$ mice, paraffin sections of livers available from mice with infiltrates were stained with polyclonal antibodies against L and H Ferritin. The immunohistochemistry staining revealed a clear separation of two zones within the infiltrate itself (Figure 3).

The liver sections labelled with anti-Fer-L revealed a visible staining of the parenchyma and a very strong labelling of the infiltrates. The Fer-L positive mononuclear infiltrate area was confined mainly to the endothelial and periendothelial region (Figure 3c). By contrast, the anti-Fer-H sections showed a heavy staining of the mononuclear cells themselves, located in the outer region of the aggregate. No strong labelling for H-Ferritin was observed in the hepatocytes (Figure 3d). Collectively, these results indicate that the mononuclear infiltrates contain both H and L ferritin.

Discussion

The results of the present comparative study between older $\beta 2m^{-/-}$ and $Hfe^{-/-}$ mice reveal the existence of differences in iron distribution, degree of iron overload, liver mononuclear cell infiltration and hepatic steatosis.

The fact that the plateau of hepatic iron concentration was reached at different ages for the $Hfe^{-/-}$ and the $\beta 2m^{-/-}$ strains (at 3.5 and 9 months, respectively) may indicate differences at the level of iron absorption. In addition, after the stabilization of hepatic iron, the $\beta 2m^{-/-}$ mice showed higher liver iron content than the $Hfe^{-/-}$ counterpart a situation that might explain results reported in other studies (Levy *et al.* 2000). Abnormally, high iron absorption has been reported both in $\beta 2m^{-/-}$ (Santos *et al.* 1998) and in the $Hfe^{-/-}$ mice (Bahram *et al.* 1999). Since none of those studies compared the two strains at the same time, in the same housing conditions, it is unclear whether they have a similar degree of iron absorption disruption. The expression profile studies carried out by Muckenthaler *et al.* (2003, 2004) in $\beta 2m^{-/-}$ and $Hfe^{-/-}$ duodenal tissue showed that both duodenal iron transporters (DMT1 and Ferroportin) are upregulated in the $\beta 2m^{-/-}$, a situation not observed in $Hfe^{-/-}$ mice. The importance of the differences seen cannot, however, be overlooked. Alternatively, the enhanced iron accumulation in $\beta 2m^{-/-}$ mice could be explained by the lack of $\beta 2m$ binding molecules, other than the Hfe itself, as concluded also by the study of Muckenthaler *et al.* (2004). Recently, it was demonstrated that the absence of classical MHC itself in mice leads to moderate hepatic iron overload (Cardoso *et al.* 2002) pointing to the importance of the MHC proteins and other unsuspected $\beta 2m$ binding molecules in iron metabolism.

In addition to the elevated liver iron content found in the $\beta 2m^{-/-}$ mice, it was apparent from the histological analysis that the hepatocytes had nuclear iron inclusions, a situation not observed in $Hfe^{-/-}$ mice, in this study, illustrated albeit not commented earlier (De Sousa *et al.* 1994).

Nuclear inclusions in hepatocytes of $Hfe^{-/-}$ mice have recently been extensively described by Magens *et al.* (2005). It must be stressed that in the present study animals were not overloaded by administration of iron. Nuclear inclusions in this and the previous report of De Sousa *et al.* (1994) iron overload developed spontaneously, thus mimicking the clinical natural history seen in human disease. Moreover, in the $\beta 2m^{-/-}$ strain, electron microscopy studies showed frequently disrupted mitochondria with an abnormal internal organization. These findings further indicate the high severity of hepatic iron overload on $\beta 2m^{-/-}$ liver when compared with the $Hfe^{-/-}$ counterpart.

The comparisons of the haematological indices from this study highlighted the differences between the mice strains at older age. With the B6 mice as baseline control, it becomes apparent that the $Hfe^{-/-}$ presents a profile resembling that seen in hemochromatosis patients, that is, normal levels of RBC counts and haemoglobin concentration and an elevated HCT, MCV and transferrin saturation. By contrast, the $\beta 2m^{-/-}$ mice showed a significantly elevated number of RBC associated with higher haemoglobin concentration as has previously been reported (8). In addition, the $\beta 2m^{-/-}$ mice presented an elevated HCT and MCV; however, the values were significantly different from those observed in the $Hfe^{-/-}$ mice. As expected both strains have elevated serum iron and transferrin saturation (Santos *et al.* 1996; Zhou *et al.* 1998). Interestingly, the TIBC observed in the $\beta 2m^{-/-}$ was higher than in control mice. That observation contrasts with the significantly lower TIBC values registered in the $Hfe^{-/-}$ strain that is normally attributed to a response to the elevated iron stores. The fact that TIBC is elevated in the $\beta 2m^{-/-}$ mice, unlike the $Hfe^{-/-}$ strain, may be due to the existence of a constitutive elevated iron absorption that surpasses the threshold of transferrin transport capacity leading to the possible mobilization of other iron binding proteins. It was recently demonstrated that haptoglobin, a plasma protein with high affinity for haemoglobin, modifies the hemochromatosis phenotype in mice, contributing significantly to iron loading observed in the $Hfe^{-/-}$ strain (Tolosano *et al.* 2005). It will be of interest to look at the circulating levels of such iron binding proteins in $\beta 2m^{-/-}$ as well as $Hfe^{-/-}$ mice.

The finding that liver steatosis was common in the $\beta 2m^{-/-}$ old mice, a situation not observed in older $Hfe^{-/-}$ or B6 mice is also of considerable interest as a model of human liver disease. Iron-storage diseases in humans are believed to cause organ damage through generation of reactive oxygen species that can cause oxidative damage to lipids. Hepatic lipid peroxidation has been demonstrated in animals with overload (by iron-supplemented diet or intraperitoneal administration of iron dextran), through the increase of major products of lipid peroxidation, such as malondialdehyde (Valerio & Petersen 1998; Khan *et al.* 2002; Sochaski *et al.* 2002) or thiobarbituric acid reactive substances, observed in 18-month-old $Hfe^{-/-}$ mice (Lebeau *et al.* 2002). In addition, it has been shown that in iron overload mice the stearyl coenzyme A desaturase 1 (SCD1) mRNA level and its corresponding activity were increased (Pigeon *et al.* 2001a). Since SCD1 is involved in the biosynthesis of unsaturated fatty acids, it was suggested that the increase of SCD1 expression and activity, could reflect a compensatory mechanism to a cellular need for renewing unsaturated fatty acids degraded by lipid peroxidation. Therefore, it is tempting to speculate

that the high hepatic iron content seen in $\beta 2m^{-/-}$ mice is linked to a pronounced lipid peroxidation in this strain. As response, lipid biosynthesis may be enhanced that in turn can lead to hepatic lipid accumulation in the form of exuberant hepatic steatosis. This was not observed in $Hfe^{-/-}$ mice.

It was also of interest that the H and L ferritin expression areas differ. The narrow perivascular, where iron accumulation has been reported in 12-month $Hfe^{-/-}$ mice (Pigeon *et al.* 2001b) was occupied by the L-fer positive mononuclear cells. It is tempting to speculate that the hepatic mononuclear cell infiltrates could be part of a response to iron load. This findings and previous results derived particularly from results with patients (Porto *et al.* 1994) and $Rag^{-/-}$ mice (Santos *et al.* 2000; Miranda *et al.* 2004) provide further evidence for an association in an experimental model of lymphocyte numbers in iron overload. However, in the experimental models, such as examined here, this conclusion is based on lymphocyte numbers from birth, examined in all compartments, whereas in patients, with a few exceptions (Cardoso *et al.* 2001) lymphocyte numbers are measured exclusively in the peripheral blood.

In conclusion, the comparison between the $Hfe^{-/-}$ and $\beta 2m^{-/-}$ mice showed that the $\beta 2m^{-/-}$ strain presents a severe hepatic iron overload picture, with higher hepatic iron content and other histocytological features such as nuclear iron inclusions and mitochondria abnormalities. The finding that liver steatosis was more common in the $\beta 2m^{-/-}$ strain may be a reflection of the high hepatic iron content causing lipid peroxidation that in turn leads to lipid biosynthesis and its accumulation. The observation that large mononuclear infiltrates were commonly observed in $Hfe^{-/-}$ strain, and not in $\beta 2m^{-/-}$, may relate to the known constitutive low number of CD8 lymphocytes in the $\beta 2m^{-/-}$ mice. Unfortunately, it was not possible to characterize the lymphocyte phenotype in the current study. The fact that these large sheets were positive for ferritin staining make it tempting to speculate that the iron sequestering capacity by lymphocytes is abrogated in $\beta 2m^{-/-}$ mice, thus contributing for a more severe progression of hepatic iron overload and steatosis in older animals of this strain.

Acknowledgements

The authors would like to thank the help of Miguel Duarte (microscopy settings), Bianca Machado (animal dissection), Cidália Silva and Júlia Reis (haematological parameters). This study was supported by the EU QLG1-CT-1999-00665 Project; Calouste Gulbenkian Foundation/FCT Project on

Hemochromatosis (Portugal) and the INNOVA Foundation/APBRF (USA).

References

- Bahram S., Gilfillan S., Kuhn L.C. *et al.* (1999) Experimental hemochromatosis due to MHC class I HFE deficiency: immune status and iron metabolism. *Proc. Natl. Acad. Sci. U. S. A.* **96**, 3312–3317.
- Cardoso E.M., Hagen K., De Sousa M., Hultcrantz R. (2001) Hepatic damage in C282Y homozygotes relates to low numbers of CD8⁺ cells in the liver lobuli. *Eur. J. Clin. Invest.* **31**, 45–53.
- Cardoso E.M., Macedo M.G., Rohrlisch P. *et al.* (2002) Increased hepatic iron in mice lacking classical MHC class I molecules. *Blood* **100**, 4239–4241.
- De Sousa M., Reimao R., Lacerda R., Hugo P., Kaufmann S.H., Porto G. (1994) Iron overload in beta 2-microglobulin-deficient mice. *Immunol. Lett.* **39**, 105–111.
- Feder J.N., Gnirke A., Thomas W. *et al.* (1996) A novel MHC class I-like gene is mutated in patients with hereditary hemochromatosis. *Nat. Genet.* **13**, 399–408.
- Herrmann T., Muckenthaler M., van der Hoeven F. *et al.* (2004) Iron overload in adult Hfe -deficient mice independent of changes in the steady-state expression of the duodenal iron transporters DMT1 and Ireg1/ferroportin. *J. Mol. Med.* **82**, 39–48.
- Khan M.F., Wu X., Tipnis U.R., Ansari G.A., Boor P.J. (2002) Protein adducts of malondialdehyde and 4-hydroxynonenal in livers of iron loaded rats: quantitation and localization. *Toxicology* **173**, 193–201.
- Lebeau A., Frank J., Biesalski H.K. *et al.* (2002) Long-term sequelae of HFE deletion in C57BL/6 \times 129/O1a mice, an animal model for hereditary haemochromatosis. *Eur. J. Clin. Invest.* **32**, 603–612.
- Levy J.E., Montross L.K., Andrews N.C. (2000) Genes that modify the hemochromatosis phenotype in mice. *J. Clin. Invest.* **105**, 1209–1216.
- Magens B., Dullmann J., Schumann K., Wulfhchel U., Nielsen P. (2005) Nuclear iron deposits in hepatocytes of iron-loaded HFE-knock-out mice: a morphometric and immunocytochemical analysis. *Acta Histochem.* **107**, 57–65.
- Miranda C.J., Makui H., Andrews N.C., Santos M.M. (2004) Contributions of beta2-microglobulin-dependent molecules and lymphocytes to iron regulation: insights from $HfeRag1^{-/-}$ and $\beta 2mRag1^{-/-}$ double knock-out mice. *Blood* **103**, 2847–2849.
- Muckenthaler M., Roy C.N., Custodio A.O. *et al.* (2003) Regulatory defects in liver and intestine implicate abnormal hepcidin and $Cybrd1$ expression in mouse hemochromatosis. *Nat. Genet.* **34**, 102–107.

- Muckenthaler M., Rodrigues P., Macedo M.G. *et al.* (2004) Molecular analysis of iron overload in B2-microglobulin-deficient mice. *Blood Dis. Mol.* **33**, 125–131.
- Pigeon C., Legrand P., Leroyer P. *et al.* (2001a) Stearoyl coenzyme A desaturase 1 expression and activity are increased in the liver during iron overload. *Biochim. Biophys. Acta* **1535**, 275–284.
- Pigeon C., Ilyin G., Courselaud B. *et al.* (2001b) A new mouse liver-specific gene, encoding a protein homologous to human antimicrobial peptide hepcidin, is overexpressed during iron overload. *J. Biol. Chem.* **276**, 7811–7819.
- Porto G., Reimão R., Gonçalves C., Vicente C., Justiça B., De Sousa M. (1994) Haemochromatosis as a window into the study of the immunological system in man: a novel correlation between CD8⁺ lymphocytes and iron overload. *Eur. J. Haematol.* **52**, 283–290.
- Rothenberg B.E. & Volland J.R. (1996) Beta2 knockout mice develop parenchymal iron overload: a putative role for class I genes of the major histocompatibility complex in iron metabolism. *Proc. Natl. Acad. Sci. U. S. A.* **93**, 1529–1534.
- Santos M., Schilham M.W., Rademakers L.H., Marx J.J., De Sousa M., Clevers H. (1996) Defective iron homeostasis in beta 2-microglobulin knockout mice recapitulates hereditary hemochromatosis in man. *Exp. Med.* **184**, 1975–1985.
- Santos M., Clevers H., De Sousa M., Marx J.J. (1998) Adaptive response of iron absorption to anemia, increased erythropoiesis, iron deficiency, and iron loading in beta2-microglobulin knockout mice. *Blood* **91**, 3059–3065.
- Santos M.M., De Sousa M., Rademakers L.H., Clevers H., Marx J.J., Schilham M.W. (2000) Iron overload and heart fibrosis in mice deficient for both beta2-microglobulin and Rag1. *Am. J. Pathol.* **157**, 1883–1892.
- Sochaski M.A., Bartfay W.J., Thorpe S.R. *et al.* (2002) Lipid peroxidation and protein modification in a mouse model of chronic iron overload. *Metabolism* **51**, 645–651.
- Tolosano E., Fagoonee S., Garuti C. *et al.* (2005) Haptoglobin modifies the hemochromatosis phenotype in mice. *Blood* **105**, 3353–3355.
- Torrance J.D. & Bothwell T.H. (1980) Tissue iron stores. In: *Methods in Hematology*, Vol. 1, pp. 104–109 (ed. J.D. Cook), New York, NY: Churchill Livingstone Press.
- Valerio L.G. Jr & Petersen D.R. (1998) Formation of liver microsomal MDA-protein adducts in mice with chronic dietary iron overload. *Toxicol. Lett.* **98**, 31–39.
- Zhou X.Y., Tomatsu S., Fleming R.E. *et al.* (1998) HFE gene knockout produces mouse model of hereditary hemochromatosis. *Proc. Natl. Acad. Sci. U. S. A.* **95**, 2492–2497.